# A Method for Producing a Shaped Contour Radiation Pattern Using a Single Shaped Reflector and a Single Feed

A.R. Cherrette and S.W. Lee
*University of Illinois*
*Urbana, Illinois*

and

R.J. Acosta
*Lewis Research Center*
*Cleveland, Ohio*

October 1988

**NASA**

A METHOD FOR PRODUCING A SHAPED CONTOUR RADIATION PATTERN

USING A SINGLE SHAPED REFLECTOR AND A SINGLE FEED

A.R. Cherrette* and S.W. Lee*
University of Illinois
Department of Electrical and Computer Engineering
Urbana, Illinois 61801

and

R.J. Acosta
National Aeronautics and Space Administration
Lewis Research Center
Cleveland, Ohio 44135

SUMMARY


Eliminating the corporate feed network in shaped countour beam antennas

will reduce the expense, weight, and RF loss of the antenna system.  One way of

producing a shaped contour beam without using a feed network is to use a single

shaped reflector with a single feed element.  For a prescribed contour beam and

feed, an optimization method for designing the reflector shape is given.  As a

design example, a shaped reflector is designed to produce a continental U. S.

coverage (CONUS) beam.  The RF performance of the shaped reflector is then

verified by physical optics.

# 1. Introduction

In many applications, spacecraft antennas require radiation patterns to be shaped such that the pattern contour fits the shape of the desired coverage region. A common example is to design the constant gain levels of the pattern to follow the projected boundary of the continental United States (CONUS) as viewed from synchronous orbit. The shaped contour radiation pattern reduces wasted transmitted power by minimizing the illumination of unwanted areas such as the ocean in this example.

The two most popular designs for producing shaped contour radiation patterns are the array fed parabolic reflector [1], [2] and the direct radiating planar array [3] (see Figures 1a and 1b, respectively). If the particular application calls for a single fixed shaped beam (no electronic scanning is needed), then both approaches generally employ passive beam-forming networks to properly weight the array elements. There are, however, several disadvantages to passive beam-forming networks. One drawback is that a major part of the cost of the antenna is in the construction and tuning of the beam-forming network; construction and tuning become more difficult as the frequency is increased. Another disadvantage is the RF loss associated with passive beam-forming networks. In general, the network loss also becomes larger with increased frequency.

It is, however, possible to generate a shaped contour radiation pattern without using a beam-forming network. This is accomplished by using a single feed element and a single shaped reflector (see Figure 1c). In this case, the far-field radiation pattern is configured to the desired shape by properly shaping the reflector surface. Using this design, a relatively inexpensive, low-

2

loss shaped beam antenna can be produced with no electrical tuning other than alignment of the feed element and reflector.

The subject of single reflector shaping for arbitrarily shaped contour beams has been an active research area since the beginning of the 1970's. One of the earliest methods consists of a wavefront synthesis technique [4]. In this method, the wavefront of the far-field radiation pattern is assumed to be composed of two parts. The inner part is a spherical wave limited in angular extent by the approximate shape of the desired coverage region. The outer part is a ruled surface with the contour of the boundary of the inner part as its directrix. The wavefront of the feed element is assumed to be spherical. The reflector surface is then completely determined from the incident and reflected wavefronts by applying the principles of geometric optics [5], [8], [9]. This method yields good results provided design parameters (such as the thickness of the outer part of the wavefront) are optimized. The design parameter optimization is necessary because there are usually differences between the desired radiation pattern and the actual radiation pattern calculated from the generated reflector surface. This difference exemplifies the difficulty of handling the geometric optics caustic associated with the outer part of the reflected wavefront.

A later method of reflector shaping replaces the wavefront synthesis with a more rigorous aperture phase synthesis [6]. In this method, the aperture phase distribution is optimized (for a fixed aperture amplitude distribution) to shape the far-field pattern. The reflector surface is then determined from the incident and reflected wavefronts in a manner similar to that given by Katagi [4].

Aperture phase synthesis eliminates the caustic problem and allows more pattern control (i.e., sidelobe suppression) than wavefront synthesis. However, one problem with aperture phase synthesis is that the aperture amplitude distribution and the aperture phase distribution cannot be independently specified (as in the case of dual shaped reflectors) [7]. The reflector shape that produces the optimized aperture phase distribution will not produce the aperture amplitude distribution assumed in the phase optimization procedure. Jorgensen in [6] uses a fixed Gaussian amplitude distribution and assumes the aperture phase has the major contribution to beam shaping. This is not a bad approximation, but it begins to break down for more complicated radiation pattern contours by causing the radiation pattern calculated from the synthesized reflector surface to be different from that for the desired radiation pattern.

To improve on the previous methods, we must find a reflector design procedure that produces an aperture amplitude and phase distribution pair that satisfies two conditions:

1)    The aperture amplitude and phase distributions produce the desired beam shape.

2)    The aperture amplitude and phase distributions can be generated by a single shaped reflector.

In this paper a method will be presented that insures that the synthesized aperture amplitude and phase distributions satisfy the above two conditions.

The synthesis method is an iterative technique that consists of three basic procedures. In the first section of this paper, the iterative technique is outlined. In the next three sections, each of the three basic procedures is described in detail. The last part of this paper applies the iterative technique to the design of a CONUS beam.

## 2. Reflector Shaping Technique

The reflector shaping technique consists of what can be conveniently thought of as the repetition of three basic procedures. Consider the reflector-feed-near-field aperture plane diagram shown in Figure 2. The first procedure is to optimize the phase distribution in the near-field aperture plane for a fixed near-field amplitude distribution. This procedure is similar to the method of [6] except that the aperture is divided into an array of square elements where each element is assumed to have uniform amplitude and phase. A least mean square phase optimization routine is then applied to find the best phase distribution for the "array" for a given amplitude distribution. The second procedure is to calculate the coordinates of the reflector surface that create the given phase distribution. As mentioned previously, the reflector surface can be completely determined from the phase distribution by applying the principles of geometric optics. The third procedure is to calculate the aperture amplitude distribution from the shaped reflector surface and feed element pattern. The new aperture amplitude distribution will be used in the next iteration of the phase optimization procedure.

Figure 3 depicts the iterative technique for determining the reflector shape. Since there must be some starting point in any iterative technique, a perfect offset parabolic reflector of an arbitrary projected aperture is chosen. This reflector produces a certain amplitude distribution that depends on the feed pattern and a uniform phase distribution. The first procedure, phase optimization, is then performed. The result is the parabolic reflector amplitude distribution combined with an optimized phase distribution that yields a far-field

radiation pattern with the desired shape. Next, the second procedure is applied and the reflector surface that produces the optimized phase distribution is determined. Once the reflector surface is known, the third procedure is performed and the new aperture amplitude distribution is obtained. From the aperture amplitude and phase information, the far-field radiation pattern of the shaped reflector can be calculated by Fourier transformation. If the far-field pattern meets the specifications, then the iterative process is ended; if not, then the new aperture amplitude distribution is used in the next iteration of the phase optimization procedure. The iterative process is then repeated until the beam shape meets the specifications, or the beam contour settles to some particular shape. The convergence of the beam shape is not guaranteed, but in practice the beam contour usually converges. This is due to the fact that the aperture phase is the dominant factor in beam shaping; the new aperture amplitude only serves to perturb the beam shaping. Consequently, the aperture phase (and thus amplitude) changes by smaller amounts as the iterative process progresses.

## 3. Phase Optimization Procedure

To formulate the phase optimization problem, consider the geometry of Figure 2. An aperture plane in front of the reflector surface is assumed to be located at $z = z_a$. The amplitude and phase of the electric field that is reflected from the reflector surface are calculated on a grid of points in the aperture plane using geometric optics [5], [9]. The aperture plane field distribution is then discretized by dividing it into square patches, where the amplitude and phase of each patch are assumed constant over the extent of the patch and equal to the value of the reference polarized electric field (i.e., $E_y$) at the center of the patch. This is essentially a two-dimensional pulse function expansion of the reference polarized aperture field, and will allow the aperture field to be treated as an array of identical elements.

The normalized reference polarized electric field component for a given direction in the far field can be written as

$$E(\theta,\phi) = \sum_{i=1}^{N} A_i \, E_i(\theta,\phi) e^{jk(x_{ai}u \, + \, y_{ai}v)} \, e^{j\beta_i} \tag{1}$$

where $E_i(\theta,\phi)$ = the normalized reference polarized electric field component (in the far field) due to the $i^{th}$ element in the aperture plane array. Unity amplitude and zero phase weighting are assumed.

$A_i$ = relative amplitude of the $i^{th}$ element

$\beta_i$ = relative phase of the $i^{th}$ element

$N$ = number of elements in the aperture

$u$ = $\sin \theta \cos \phi$

8

$$v = \sin \theta \sin \phi$$

$x_{ai}$ = the x coordinate of the $i^{th}$ element

$y_{ai}$ = the y coordinate of the $i^{th}$ element

Note that the normalization is such that the gain in dBi of the $i^{th}$ element is given by

$$Gain_i(\theta,\phi) = 10 \log_{10} (|E_i(\theta,\phi)|^2) \tag{2}$$

The gain of the array can then be approximated as

$$Gain(\theta,\phi) = \frac{|E(\theta,\phi)|^2}{\sum\limits_{i=1}^{N} A_i^2} \tag{3}$$

Here it is assumed that the power radiated by each individual isolated element can be added to obtain the power radiated by the array.

If (3) is parameterized such that gain in the $j^{th}$ direction of interest in the far field is denoted by

$$Gain(\theta_j,\phi_j) = \frac{|E(\theta_j,\phi_j)|^2}{\sum\limits_{i=1}^{N} A_i^2} = \frac{|E_j|^2}{\sum\limits_{i=1}^{N} A_i^2} = G_j \tag{4}$$

where 
$$E_j = \sum_{i=1}^{N} A_i E_{ij} e^{j\beta_i}$$

$$E_{ij} = E_i(\theta_j,\phi_j) e^{jk(x_{ai}u_j + y_{ai}v_j)}$$

then a cost function $\psi$, that is always positive, can be defined as

$$\psi = \sum_{j=1}^{M} |G_j - GD_j|^2 \tag{5}$$

where $GD_j$ = the gain desired in the $j^{th}$ direction of interest

$M$ = number of far-field directions where gain is to be optimized.

Minimizing $\psi$ is the criterion for the optimization procedure. Note that when $\psi$ is minimized, the mean square difference between the gain desired and the gain achieved is minimized. For phase optimization, the set of phases $\beta_i$ that minimize $\psi$ is sought.

The set of $\beta_i$ that minimizes $\psi$ can be found by applying the method of steepest descent. The method takes the following form

$$\begin{bmatrix} \beta_1(k+1) \\ \beta_2(k+1) \\ \cdot \\ \cdot \\ \cdot \\ \beta_N(k+1) \end{bmatrix} = \begin{bmatrix} \beta_1(k) \\ \beta_2(k) \\ \cdot \\ \cdot \\ \cdot \\ \beta_N(k) \end{bmatrix} - \mu \begin{bmatrix} \dfrac{\partial \psi}{\partial \beta_1} \Big| \beta_1 = \beta_1(k) \\ \dfrac{\partial \psi}{\partial \beta_2} \Big| \beta_2 = \beta_2(k) \\ \cdot \\ \cdot \\ \dfrac{\partial \psi}{\partial \beta_N} \Big| \beta_N = \beta_N(k) \end{bmatrix} \tag{6}$$

where $\beta_i(k) = \beta_i$ on the $k^{th}$ iteration of the algorithm of (6). By properly choosing $\mu$, $\psi$ will be minimized since the gradient (the last term on the right of (6)) gives the direction in $\beta$-space that results in the greatest increase in $\psi$ (see Figure 4). A method for choosing $\mu$ that works fairly well in practice is to first set $\mu$ equal to the inverse of the magnitude of the gradient in (6), then reduce $\mu$ by an additional 0.9 times every time the cost function increases.

10

The gradient can be easily calculated since $\psi$ is an explicit function of $\beta_i$. The result is

$$\frac{\partial \psi}{\partial \beta_i} = \sum_{j=1}^{M} 2[G_j - GD_j] \frac{1}{\sum_{i=1}^{N} A_i^2} [jA_i E_{ij} e^{j\beta_i} E_j^* - jA_i E_{ij}^* e^{-j\beta_i} E_j] \qquad (7)$$

Note that the gradient is also a function of the particular set of $A_i$, i=1, N used in the procedure.

By starting with initial phase and amplitude distributions, $\beta_i(0)$ and $A_i(0)$ i=1,N, a new phase distribution, $\beta_i(k)$ i=1,N, ($A_i(0)$ i=1,N remain unchanged) is obtained that minimizes the mean square difference between the gain desired and the gain achieved at the various far-field directions. By choosing the desired gains and their corresponding directions to cover the area of interest (CONUS, for example), a shaped contour radiation pattern can be produced. Note that sidelobes can be suppressed in selected directions by choosing the gain desired to be small for those directions.

The choice of the least mean square optimization criterion (5), (6) is arbitrary. The beam shaping method could also employ a minimax algorithm as long as phase is the only optimized variable.

11

## 4.  Calculation of the Reflector Surface

Once the optimized aperture phase distribution is known, a reflector surface can be completely determined from this distribution by applying the principles of geometric optics.  Consider the geometry of Figure 5.  If one reflection point, A, on the reflector surface is assumed to be known, then the length of what will be referred to as the reference path, d, is known and given by

$$d = | \vec{FA} | + | \vec{AA}_a |$$
(8)

where       F denotes the feed position at (0, 0, f)

               $A_a$ denotes a point in the aperture plane.

Note that the incident ray $\vec{FA}$ produces the reflected ray $\vec{AA}_a$, and the total length along this ray path is given by the reference path length.  For any other point P on the reflector surface, the length of the ray path d' is given by

$$d' = |\vec{FP}|+|\vec{PP}_a| = \left[ x^2 + y^2 + (z-f)^2 \right]^{1/2} + \left[ (x-x_a)^2 + (y-y_a)^2 + (z-z_a)^2 \right]^{1/2}$$
(9)

where       $P_a$ denotes a point in the aperture plane $(x_a, y_a, z_a)$

               P denotes a point on the reflector (x, y, z).

In this case the incident ray $\vec{FP}$ produces the reflected ray $\vec{PP}_a$.  If it is assumed that the phase in the aperture plane is continuous and that the phases at points $A_a$ and $P_a$ in the aperture plane are given by $\theta(A_a)$ and $\theta(P_a)$, respectively, then the following relation holds

$$d' = \frac{-1}{k} \left[ \theta(P_a) - \theta(A_a) \right] + d$$
(10)

12

where $\quad k = \dfrac{2\pi}{\lambda}$

Equation (10) relates the length difference between the two ray paths to the difference in their corresponding phase values in the aperture plane. The right-hand side of (10) is known and the left-hand side contains the unknowns x, y, and z, the coordinates of a point on the reflector surface which remains to be determined. Two more independent equations are needed to solve for the three unknowns. These two equations are obtained from the expression for the line passing through the points P and $P_a$. In the geometric optics limit, the ray $\vec{PP}_a$ is normal to the equiphase surface and parallel to the wave vector $\vec{k}$ at the point $P_a$. More precisely

$$\frac{\vec{PP}_a}{|\vec{PP}_a|} = \frac{\vec{k}}{k}\Bigg|_{P_a} = \frac{1}{k}\left(k_x\,\hat{x} + k_y\,\hat{y} + k_z\,\hat{z}\right)\Bigg|_{P_a} = \frac{1}{k}\,\nabla\theta\,(x,\,y,\,z)\Bigg|_{P_a} \qquad (11)$$

where $\quad |\vec{k}| = k = \dfrac{2\pi}{\lambda}$

Therefore, the two equations for the line passing through $\vec{PP}_a$ are given by

$$\frac{x-x_a}{m_x} = \frac{z-z_a}{m_z} \qquad\qquad\qquad\qquad (12)$$

$$\frac{y-y_a}{m_y} = \frac{z-z_a}{m_z} \qquad\qquad\qquad\qquad (13)$$

where $\quad m_x = \dfrac{k_x}{k}\Bigg|_{P_a} = \dfrac{1}{k}\dfrac{\partial\theta}{\partial x}\Bigg|_{P_a} \qquad\qquad (14a)$

$$m_y = \frac{k_y}{k}\Bigg|_{P_a} = \frac{1}{k}\frac{\partial\theta}{\partial y}\Bigg|_{P_a} \qquad\qquad (14b)$$

13

$$m_z = \left[ 1 - m_x^2 - m_y^2 \right]^{1/2} \tag{14c}$$

Since the phase distribution in the aperture plane is known, the partial derivatives of the phase with respect to x and y can be approximated by difference expressions. The only unknowns in Equations (12) and (13) are x, y, and z. Therefore, Equations (10), (12) and (13) can then be solved for the three unknowns (x, y, z) yielding a point on the reflector surface. The solution of the three equations is given by

$$z = \frac{Q^2(x_a, y_a) - x_a^2 - y_a^2 - z_a^2 + 2z_a f - f^2}{2(\sigma x_a + \gamma y_a + z_a - f) - 2Q(x_a, y_a)(\sigma^2 + \gamma^2 + 1)^{1/2}} - z_a \tag{15a}$$

$$y = \gamma (z - z_a) + y_a \tag{15b}$$

$$x = \sigma (z - z_a) + x_a \tag{15c}$$

where

$$Q(x_a, y_a) = \frac{1}{k} \left[ \theta(A_a) - \theta(P_a) \right] + d$$

$$\gamma = \frac{m_y}{m_z}$$

$$\sigma = \frac{m_x}{m_z}$$

At the beginning of this derivation two variables were assumed to be known, d, $\theta(A_a)$. These variables are chosen arbitrarily as

$$d = f + z_a \tag{16a}$$

$$\theta(A_a) = 0 \tag{16b}$$

where f is the focal length of the initial parabolic reflector that is used to begin the iterative surface shaping technique and $z_a = 0$ is the equation of the

aperture plane. Note also that the solutions of (10), (12) and (13) automatically satisfy Snell's law for smooth phase distributions [8].

It should be mentioned that if there are discontinuities in the aperture phase distribution, the corresponding reflector surface points will not satisfy Snell's law. Since, for every point in the aperture plane, a reflection point on the reflector surface is determined, a normal for every reflector point can be determined from neighboring reflection points. In this way, Snell's law can be tested. It will be shown that discontinuities in the aperture phase will produce discontinuities in the reflector surface.

## 5. Calculation of the Aperture Plane Amplitude Distribution

After the surface has been determined at a discrete set of points, the aperture amplitude distribution can be calculated. All points on the reflector surface can be tested to see if Snell's law is satisfied. For those points that satisfy Snell's law, the amplitude of the exit ray can be calculated in the aperture plane by the projected area ratio of a ray tube (see Figure 6). It is well known [5], [9] that

$$|E_a| = |E_r| \sqrt{\frac{Area_1}{Area_2}} \tag{17}$$

where

$|E_r|$ = magnitude of the reflected field at the reflector surface

$|E_a|$ = magnitude of the reflected field in the aperture plane

$Area_1$ = projected area of the ray tube at the reflector surface

$Area_2$ = projected area of the ray tube in the aperture plane.

A small ray tube can be formed by selecting three rays in close proximity. Consider Figure 6; the three incident rays are $\vec{F}P(I,J)$, $\vec{F}P(I+1,J)$ and $\vec{F}P(I,J+1)$. The corresponding reflected rays are $\overrightarrow{P(I,J)\vec{P}_a}(I,J)$, $\overrightarrow{P(I+1,J)\vec{P}_a}(I+1,J)$ and $\overrightarrow{P(I,J+1)\vec{P}_a}(I,J+1)$. As the aperture points and the reflection points are brought closer together, (17) can be used to approximate the aperture field $E_a$ at point $P_a(I,J)$. The approximation becomes exact as the areas go to zero. The projected areas are given by (see Figure 7)

$$Area_1 = \frac{1}{2} h \cdot side\ 1 * \hat{k}_i \cdot \hat{n} \tag{18}$$

where

$$h = side\ 2 * \sqrt{1-(\cos \alpha)^2}$$

$$\cos \alpha = \frac{(side\ 3)^2 - (side\ 1)^2 - (side\ 2)^2}{2(side\ 1) * (side\ 2)}$$

16

$$\text{side } 1 = \mid P(I,J) - P(I+1,J) \mid$$

$$\text{side } 2 = \mid P(I,J) - P(I,J+1) \mid$$

$$\text{side } 3 = \mid P(I+1,J) - P(I,J+1) \mid$$

$\hat{k}_i$ = normalized incident ray direction

$\hat{n}$ = normal to the surface at $P(I,J)$

$$\text{Area}_2 = \frac{1}{2} * \text{cell} * \hat{k}_r \cdot \hat{z} \tag{19}$$

cell = area of square patch in aperture

$\hat{k}_r$ = normalized reflected ray direction

$\hat{z}$ = normal to aperture plane

The field quantity $\mid E_r \mid$ in (17) is known from the given primary feed pattern; therefore, the amplitude distribution in the aperture can be calculated from (17).

## 6. Design of a CONUS Beam

The iterative technique outlined in the previous sections was used to design a CONUS shaped contour radiation pattern. To begin the design procedure, 73 directions in the far field were chosen to cover the projected CONUS map as viewed from a particular synchronous orbit position as shown in Figure 8. Next, an initial offset parabolic reflector and feed element were selected for the starting point of the iterative process. This reflector and feed are shown in Figure 9, and the far-field pattern is shown in Figure 10. The amplitude and phase of the reference polarized electric field component were then calculated over the aperture plane on a 47 by 47 point square grid. The resulting 2209 square patches (elements) in the aperture plane were each 0.543 λ on a side. The normalized reference polarized electric field component due to each patch was calculated in each of the 73 far-field directions. The field component due to each of the 2209 aperture elements in each of the 73 far-field directions forms the data base for the phase optimization procedure.

The three basic procedures - phase optimization, reflector surface calculation, and aperture amplitude distribution calculation - were performed using the initial aperture amplitude and phase distributions for the perfect parabolic reflector. From the resultant new aperture amplitude and phase distributions (and corresponding reflector surface), the far-field pattern shown in Figure 11 was obtained. The beam shape is beginning to take on the CONUS form, but the process needs to be continued to improve the beam shape.

The three basic procedures were then repeated for a second iteration with the aperture amplitude and phase that produced the far-field pattern shown in

18

Figure 11 as input. The resultant aperture amplitude and phase after the second iteration produced the far-field pattern shown in Figure 12. The procedures were again repeated for a third iteration, and the far-field pattern of Figure 13 was produced from the resultant shaped reflector surface (and corresponding aperture amplitude and phase). After the fourth iteration, the far-field pattern of Figure 14 was obtained. The far-field pattern did not change much when going from the third to the fourth iteration so the iterative process was ended. The final aperture amplitude distribution and aperture phase distribution are shown in Figures 15 and 16, respectively. The final shaped reflector surface is shown in Figures 17 and 18. The cross-polarization pattern after the fourth iteration is shown in Figure 19. (The feed model had no cross-polarized component.) The gain over the coverage region was greater than 28.0 dBi with the polarization isolation less than -26 dB.

Note that the difference between the shaped surface and the parabolic surface is almost saddle shaped with slight discontinuities in the surface in the steep portions of the saddle shape. Notice similar discontinuities in the phase distribution. These discontinuities were detected by testing to see if Snell's law was satisfied. At the discontinuity points (edge points) the reflected fields were neglected when calculating the far-field pattern. The electrical performance of the shaped reflector was checked by applying physical optics. Figure 20 shows the physical optics far-field radiation pattern for the interpolated shaped reflector surface of Figure 18. Note there is very little difference between the physical optics pattern and the geometric optics pattern of Figure 14.

## 7. Conclusion


A method has been presented for synthesizing a single reflecting surface that accurately produces a shaped contour radiation pattern when the radiation contour shape and feed pattern are specified. The method is quite general in that it will take into account discontinuities in the reflecting surface. Results were generated for a CONUS beam design, and very good beam shaping resulted. The electrical performance of the shaped reflector surface was also verified by physical optics.

REFERENCES

[1]   A. W. Rudge, K. Milne, A. D. Olver and P. Knight, The Handbook of Antenna
      Design, vol. 1. sect. 3.5, London: Peter Peregrinus, Ltd., 1982.

[2]   W. V. T. Rusch, "The current state of the reflector antenna art," IEEE
      Trans. Antennas Propagat., vol. AP-32, pp. 313-329, 1984.

[3]   A. R. Cherrette and D. C. D. Chang, "Phased array contour beam shaping by
      phase optimization," Antennas Propagat. Symp. Int. Symp. Digest.,
      Vancouver, B.C., 1985, pp. 475-478.

[4]   T. Katagi and Y. Takeichi, "Shaped-beam horn-reflector antennas," IEEE
      Trans. Antennas Propagat., vol. AP-23, pp. 752-763, 1975.

[5]   P. H. Pathak, "Techniques for high frequency problems," Antenna Handbook,
      Ch. A7, Y. T. Lo and S. W. Lee, Eds. New York: Van Nostrand Reinhold Co.
      Inc., 1988.

[6]   R. Jorgensen, "Coverage shaping of contoured-beam antennas by aperture
      field synthesis," Proc. IEE, vol. 127, pp. 201-208, 1980.

[7]   B. S. Westcott, Shaped Reflector Antenna Design.  Letchworth, England:
      Research Studies Press, 1983, pp. 79-82.

[8]   R. E. Collin and F. J. Zucker, Antenna Theory, part 2.  New York:  McGraw
      Hill, 1969, pp. 21-23, 33-34.

[9]   S. W. Lee, "Electromagnetic reflection from a conduction surface:
      geometrical optics solution," IEEE Trans. Antennas Propagat., vol. AP-23,
      pp. 184-191, 1975.
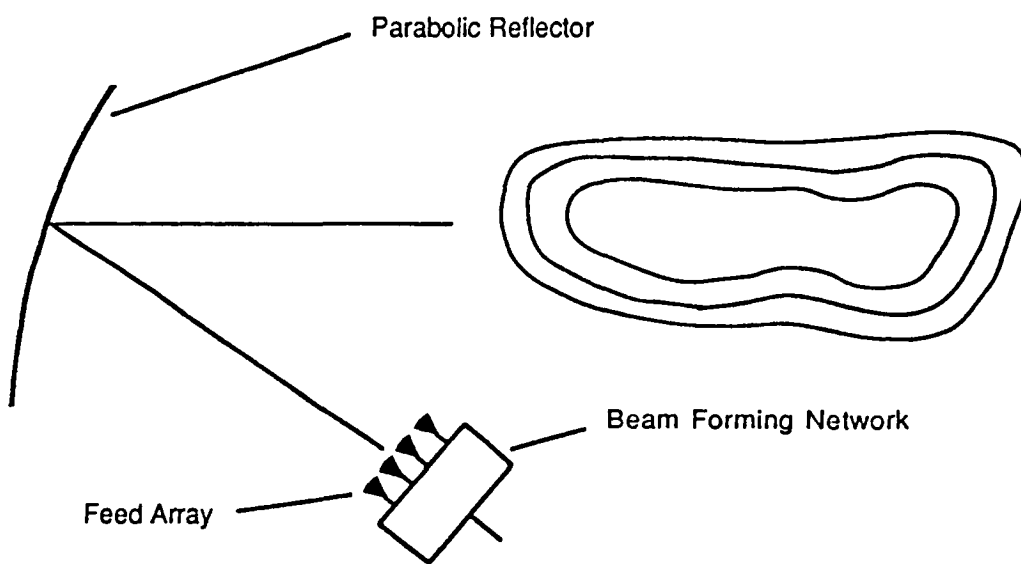
FIGURE 1a.   Parabolic Reflector with an Array Feed

Planar Array

Beam Forming Network
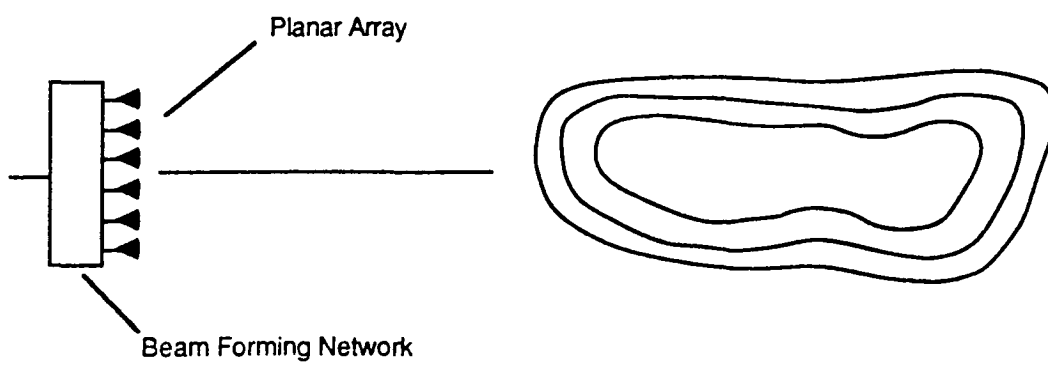
**FIGURE 1b.  Direct  Radiating  Planar  Array**

Single Shaped Reflector
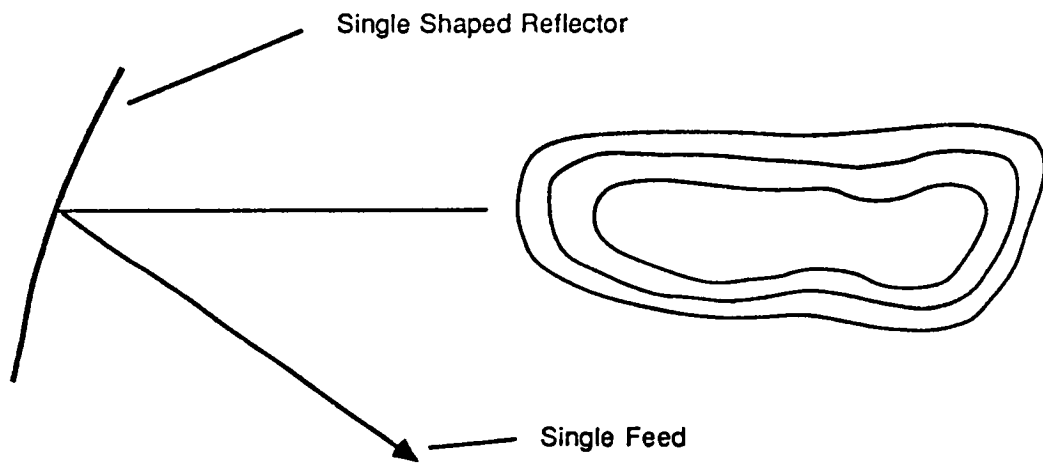
Single Feed

FIGURE 1c.   Single Shaped Reflector with a Single Feed

Reflector

Aperture Plane

Element in
Aperture Plane

Feed
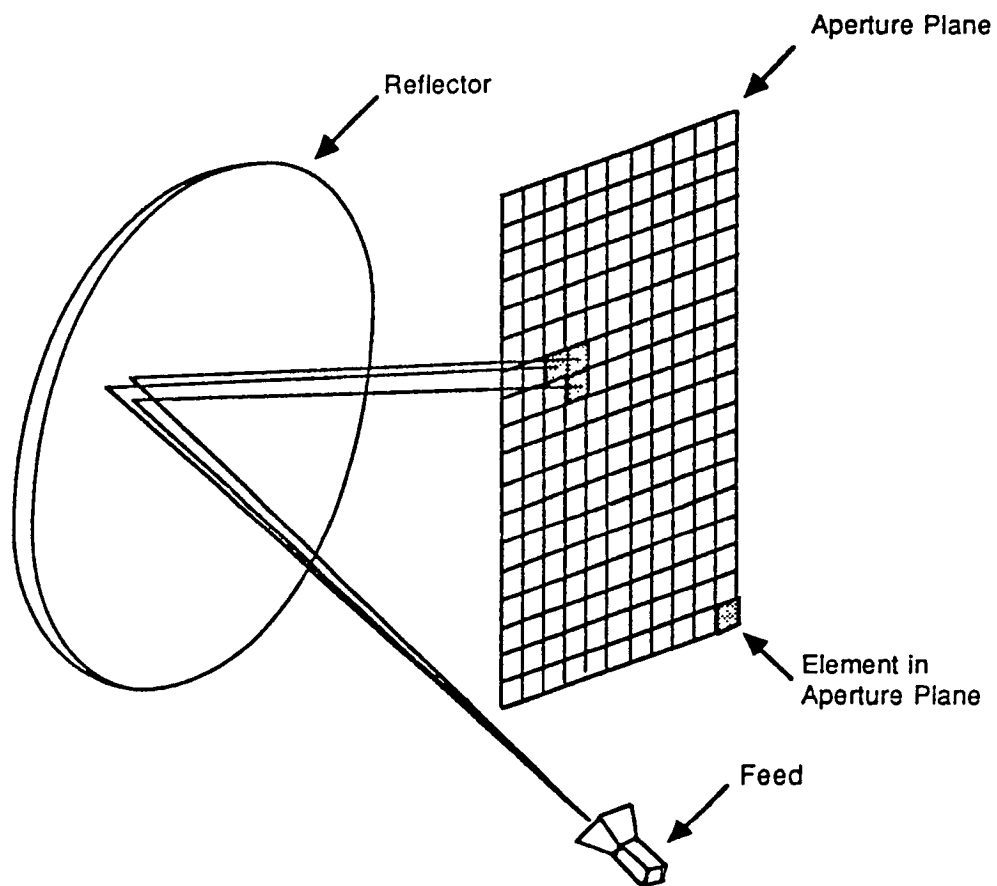
**FIGURE 2. Geometry of the Reflector Shaping Problem**

Reflector
Surface

Amplitude
Distribution

Phase
Distribution

Phase Optimization

Reflector Surface Calculation

Nearfield Amplitude Calculation

Phase Optimization
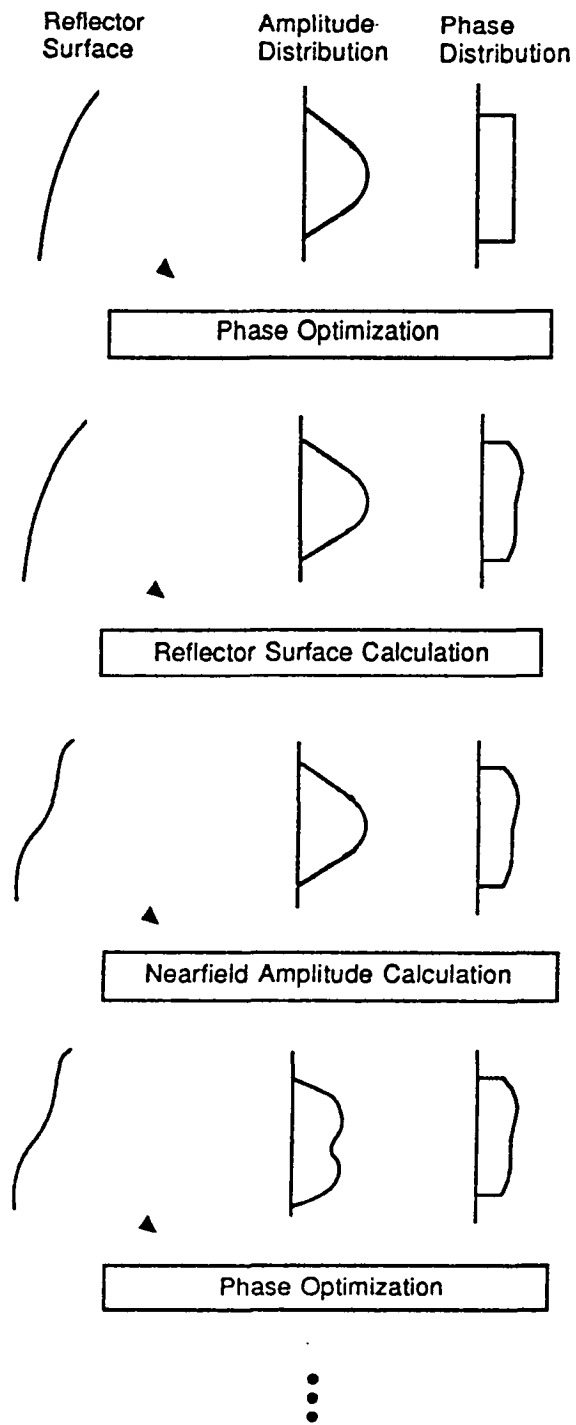
FIGURE 3. Iterative Reflector Shaping Technique
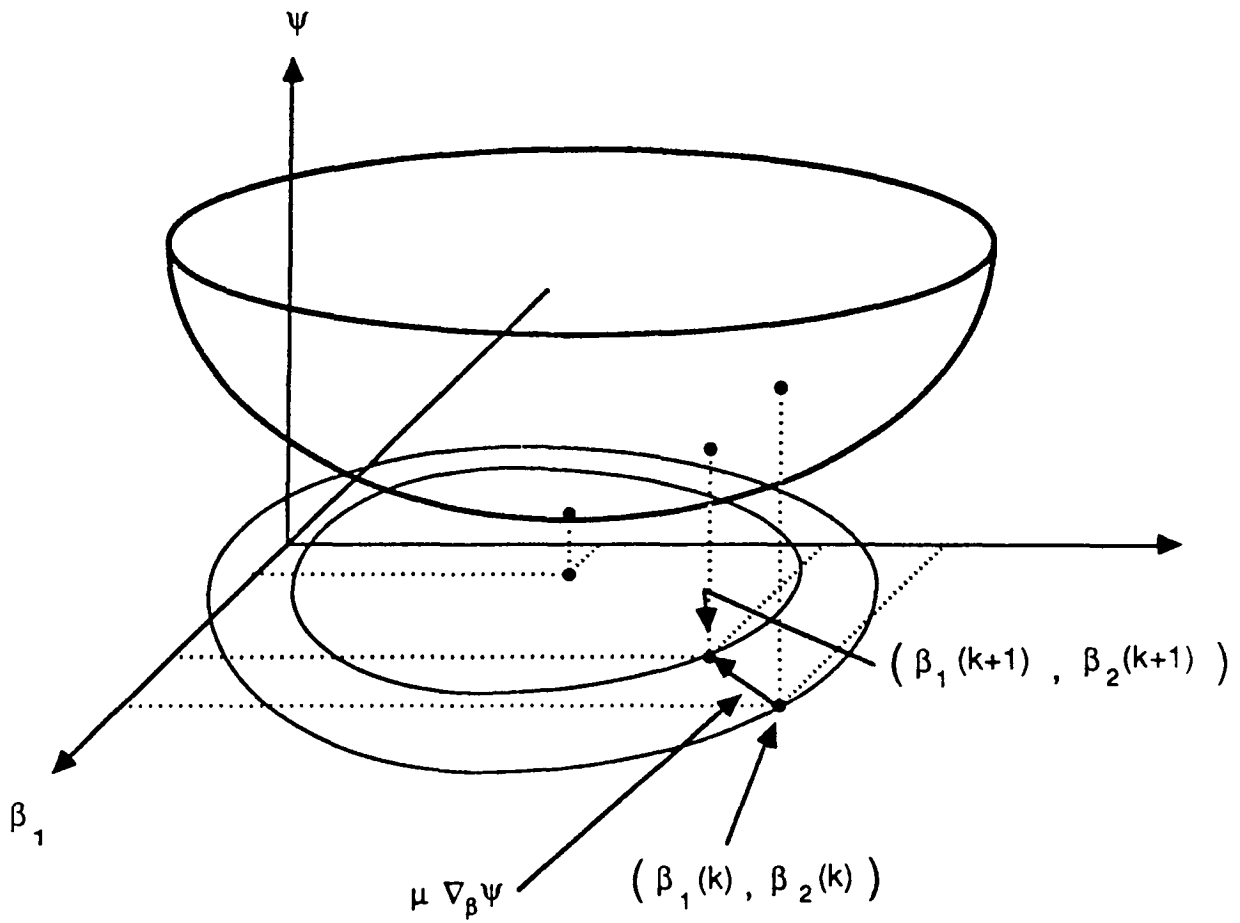
FIGURE 4. Three Dimensional Illustration of the Cost Function,
$\Psi$, as a Function of Two Phase Variables, $\beta_1$ and $\beta_2$
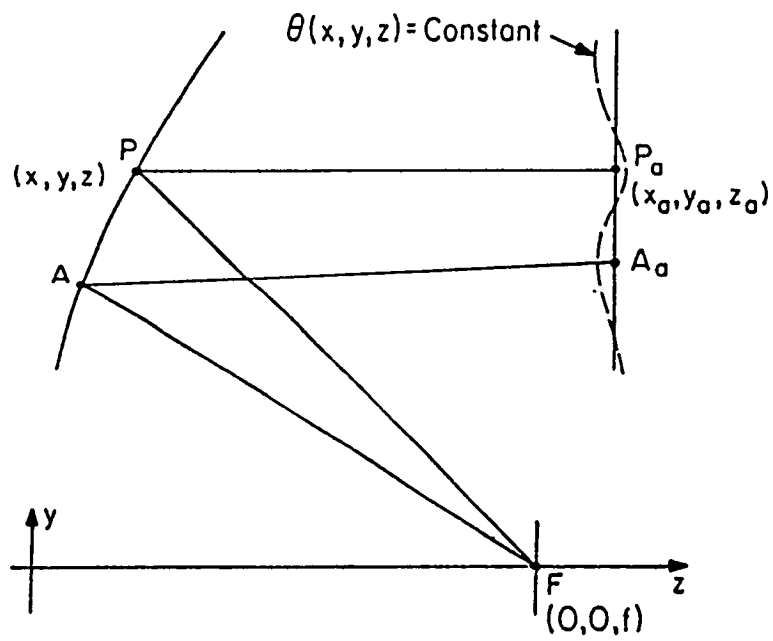
FIGURE 5.  Geometry for the Surface Calculation

P (I,J)

P (I+1,J)

P (I,J+1)

$P_a$ (I,J)

$P_a$ (I,J+1)

$P_a$ (I+1,J)

F
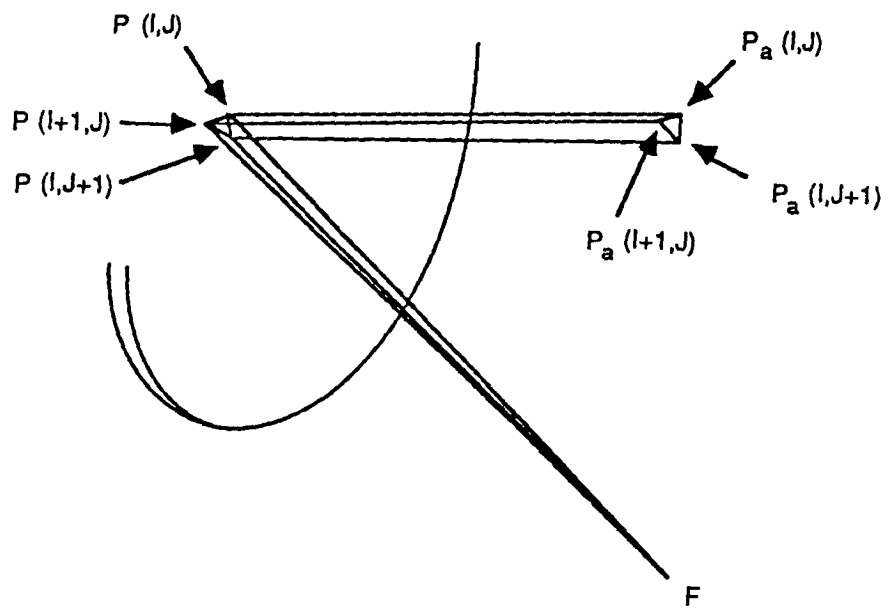
FIGURE 6. Incident and Reflected Ray Tubes
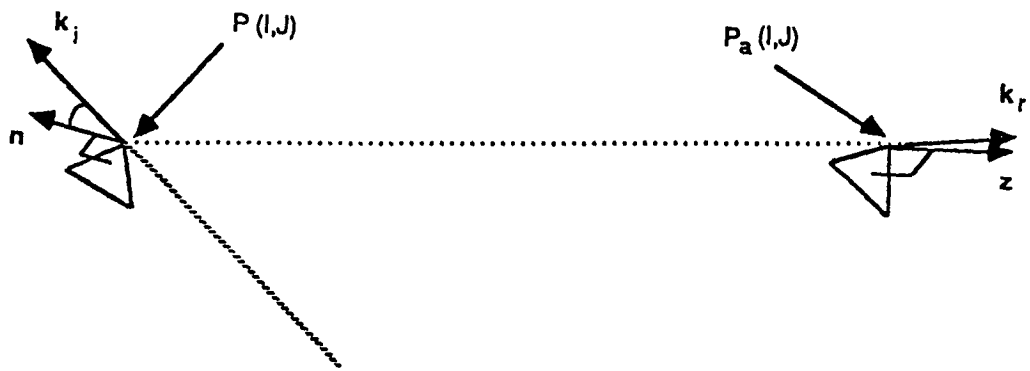
**FIGURE 7.** Cross Sections of the Ray Tubes at the Reflector and in the Aperture Plane
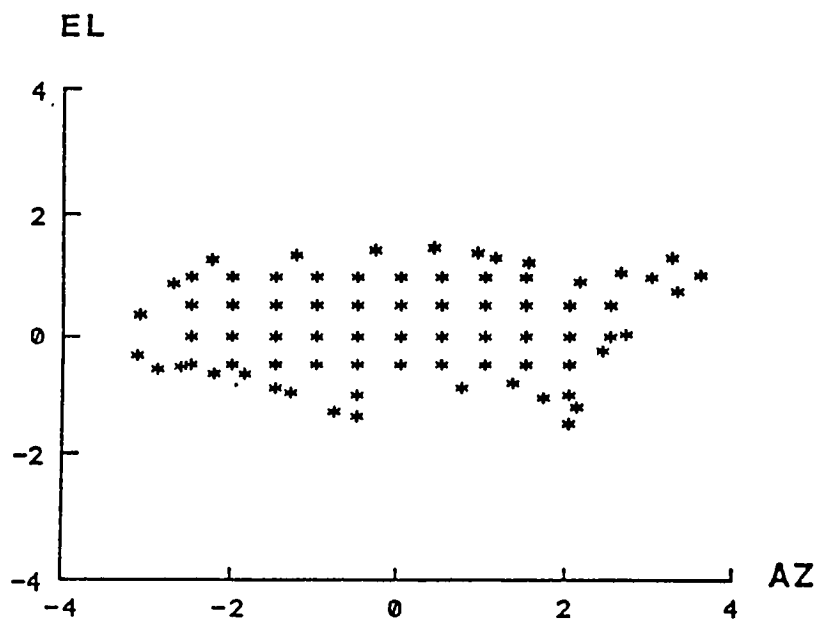
**FIGURE 8.** Farfield Points Over which Gain is Optimized
(Desired Gain > 28 dBi for all Points)

Nearfield Aperture

$Z_A$

$R$

$H$

F
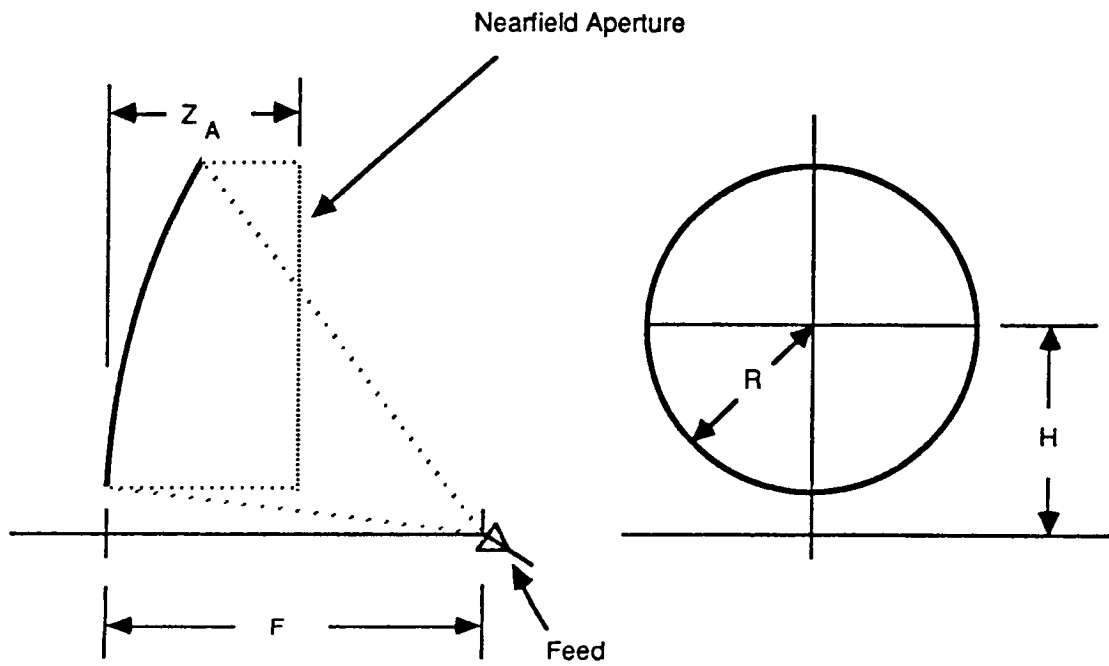
Feed

$F = 25.0\ \lambda$            $R = 12.5\ \lambda$

$Z_A = 14.0\ \lambda$            $H = 15.5\ \lambda$

Feed Pattern : E - Plane ..... $\cos^q \theta$

H - Plane ..... $\cos^q \theta$

$q = 11.25$

FIGURE 9.    Geometry of the Initial Parabolic Reflector
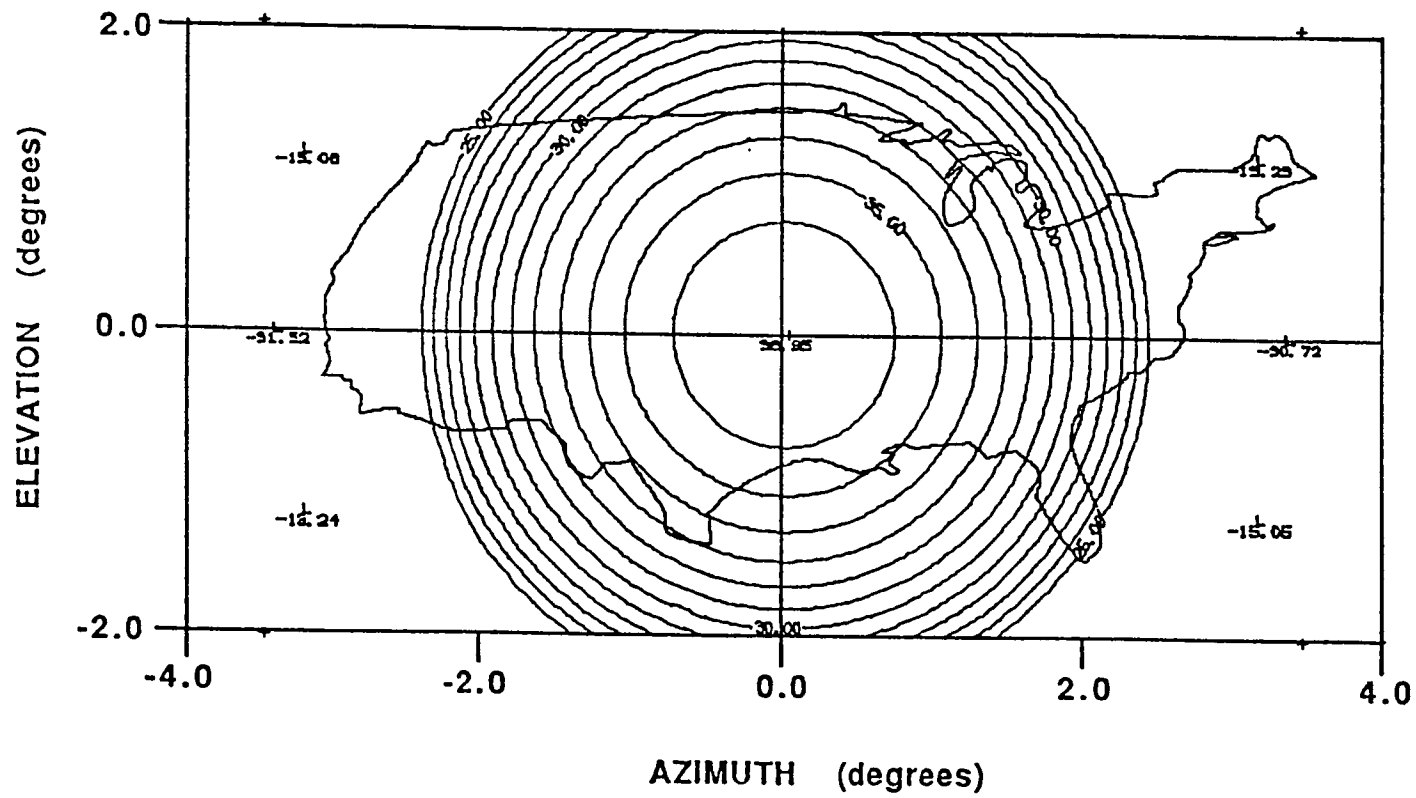
FIGURE 10. Far Field Pattern for the Initial Parabolic Reflector
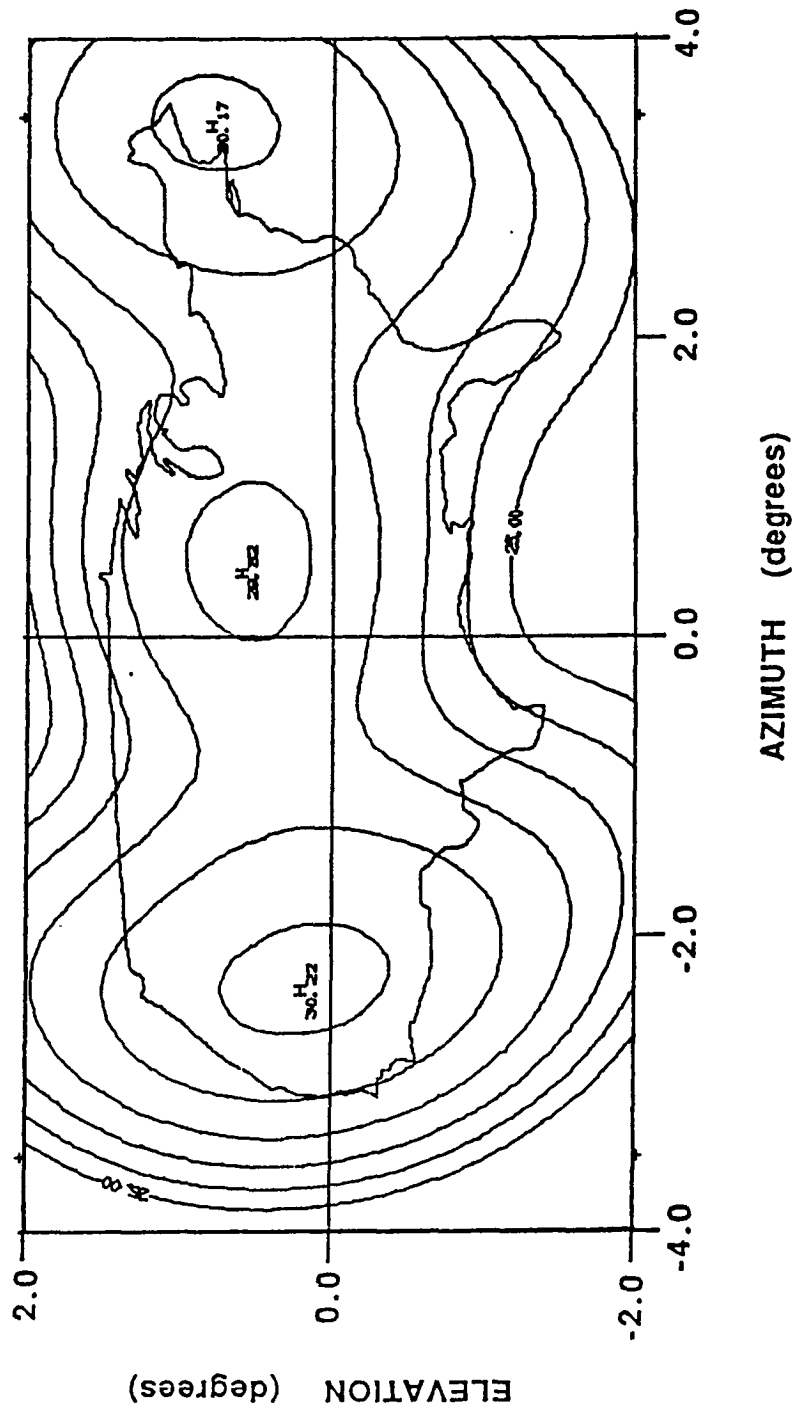
FIGURE 11. Far Field Pattern for the Shaped Reflector after the First Iteration
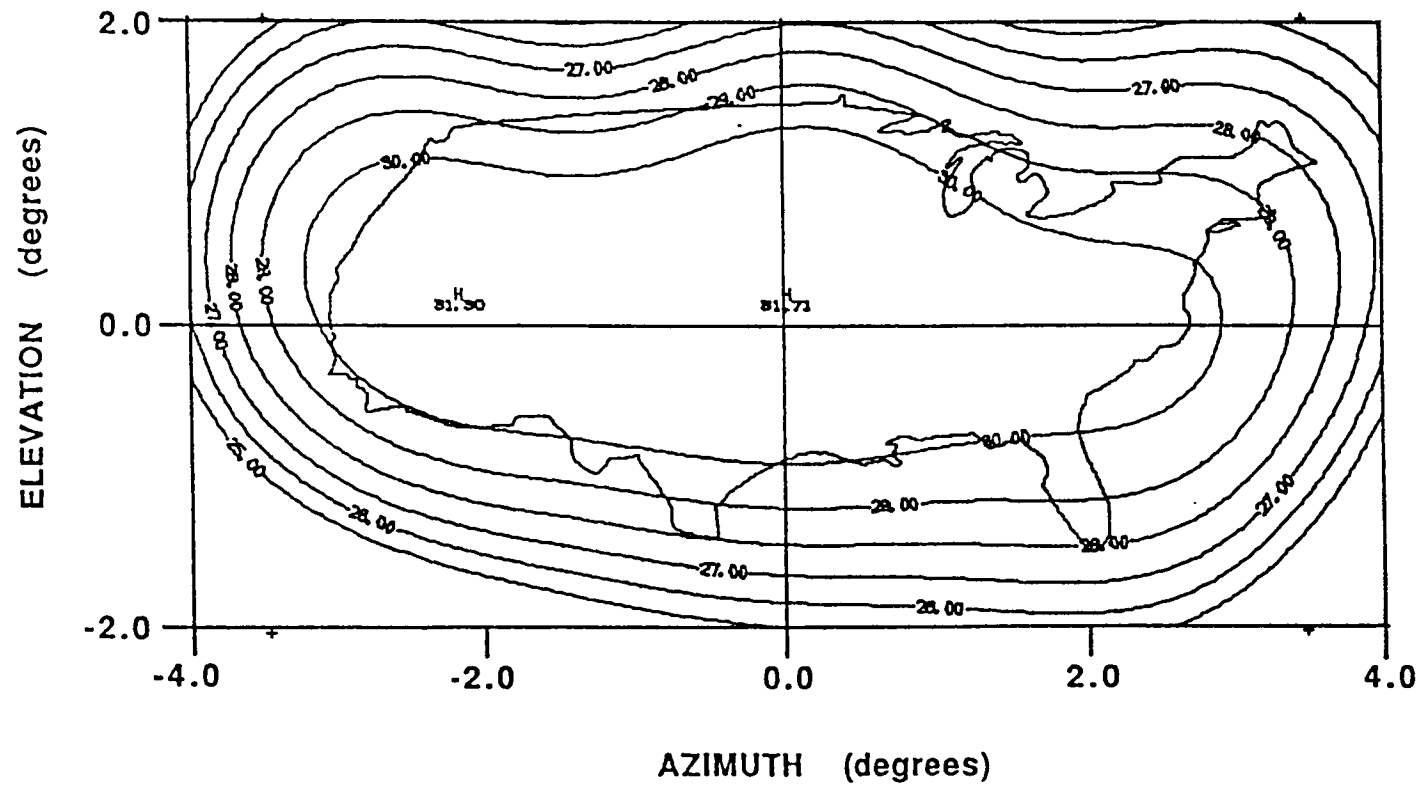
FIGURE 12. Far Field Pattern for the Shaped Reflector after the Second Iteration

ELEVATION (degrees)
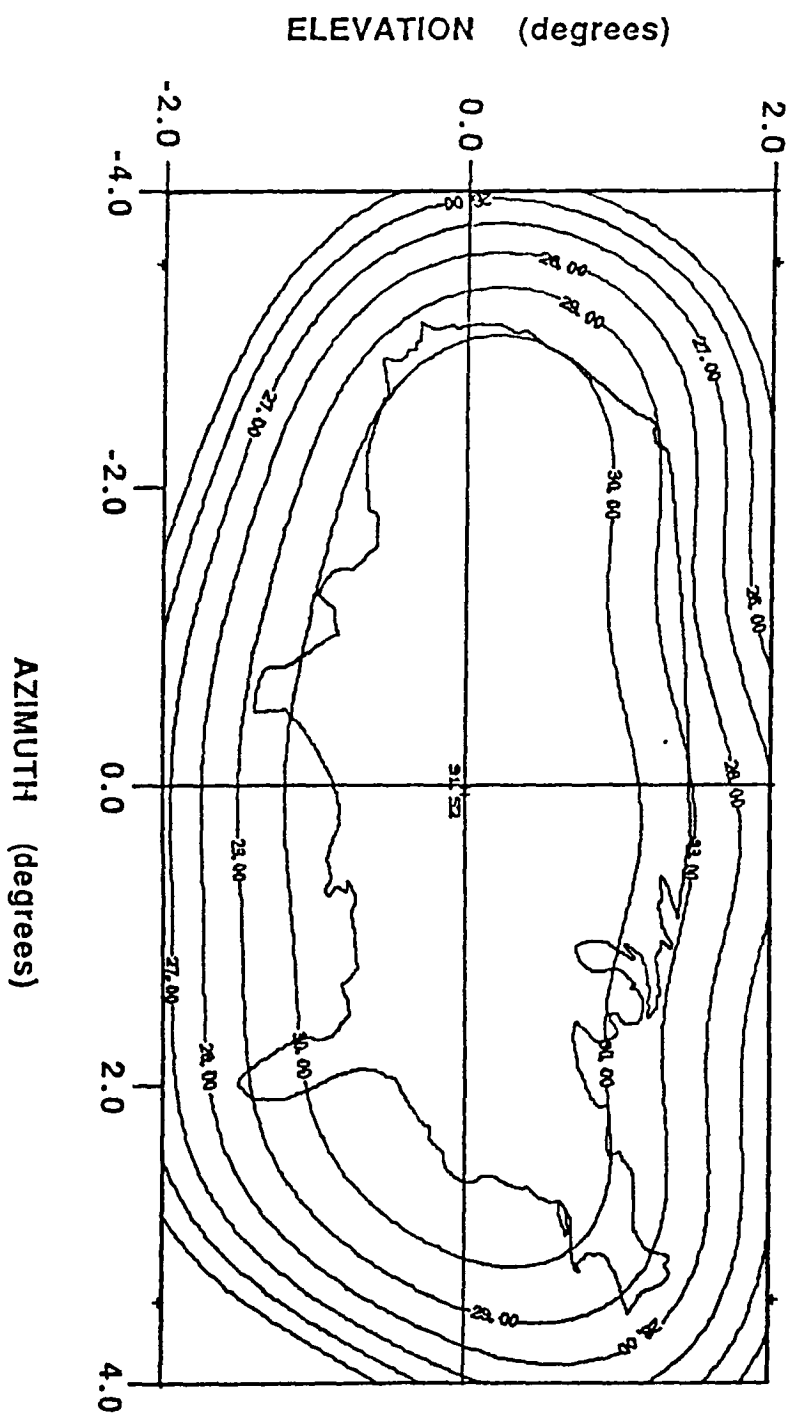


FIGURE 13. Far Field Pattern for the Shaped Reflector after the Third Iteration

AZIMUTH (degrees)
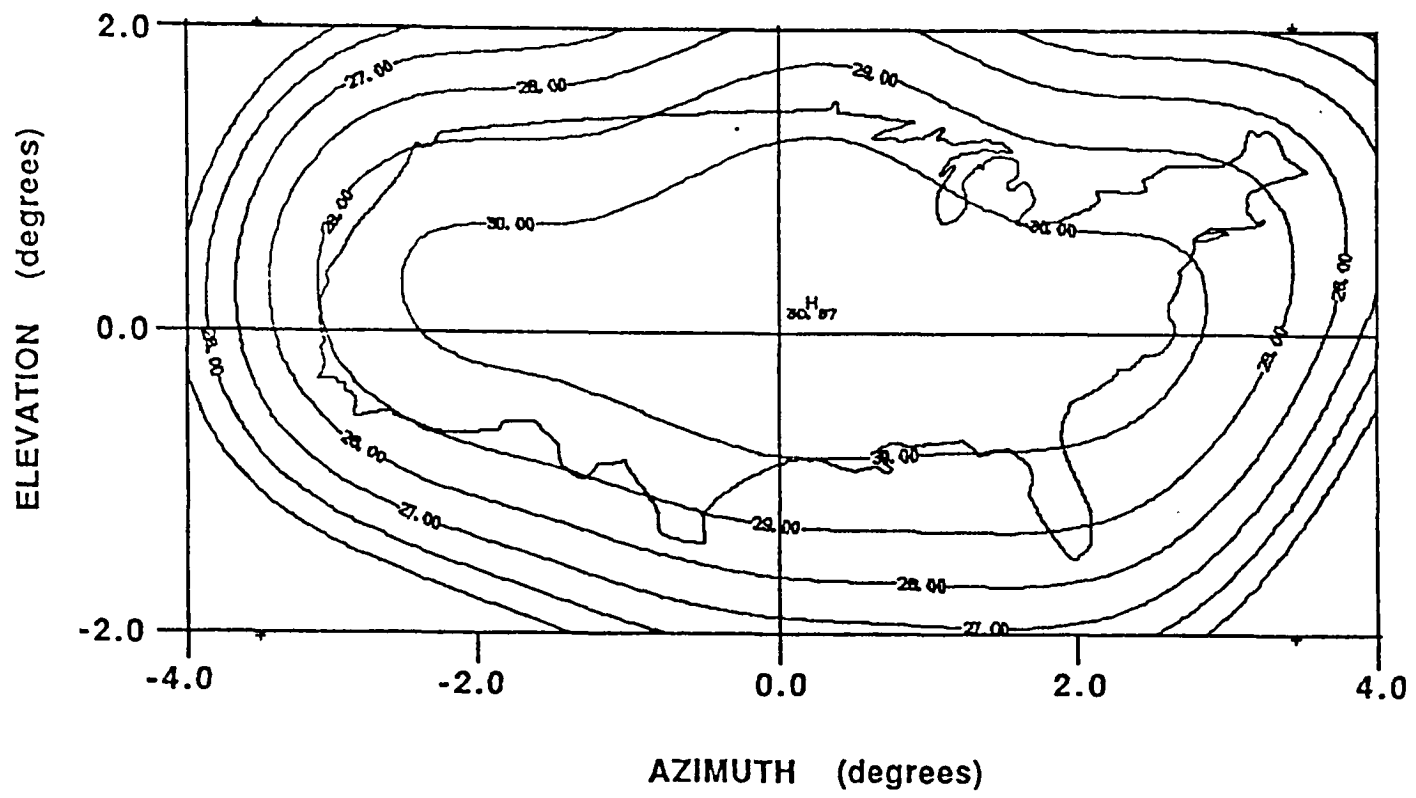
**FIGURE 14. Far Field Pattern for the Shaped reflector after the Fourth Iteration.** The antenna gain is greater than 28.0 dBi over the coverage area.
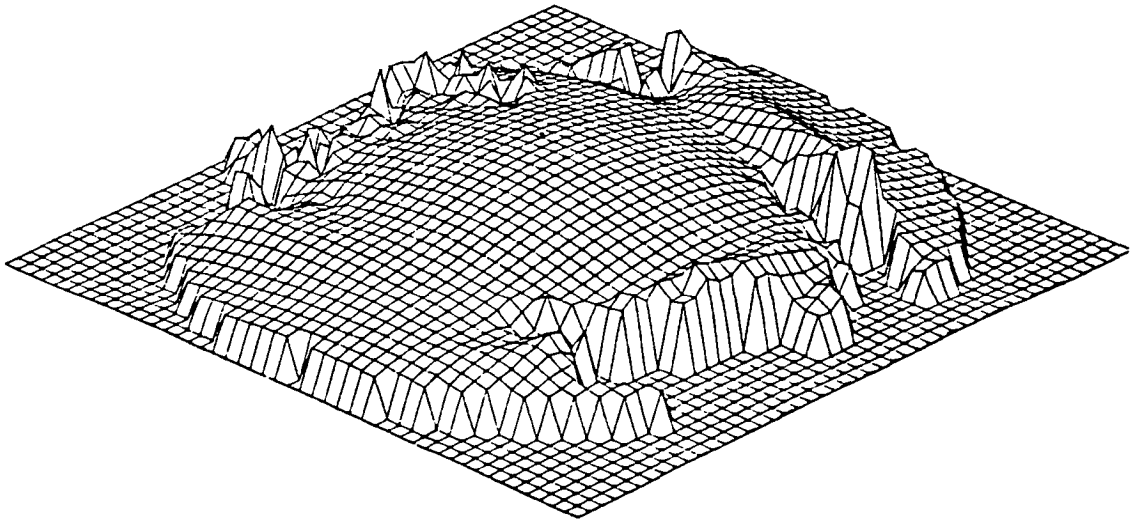
FIGURE 15. Aperture Amplitude Distribution after the
Fourth Iteration
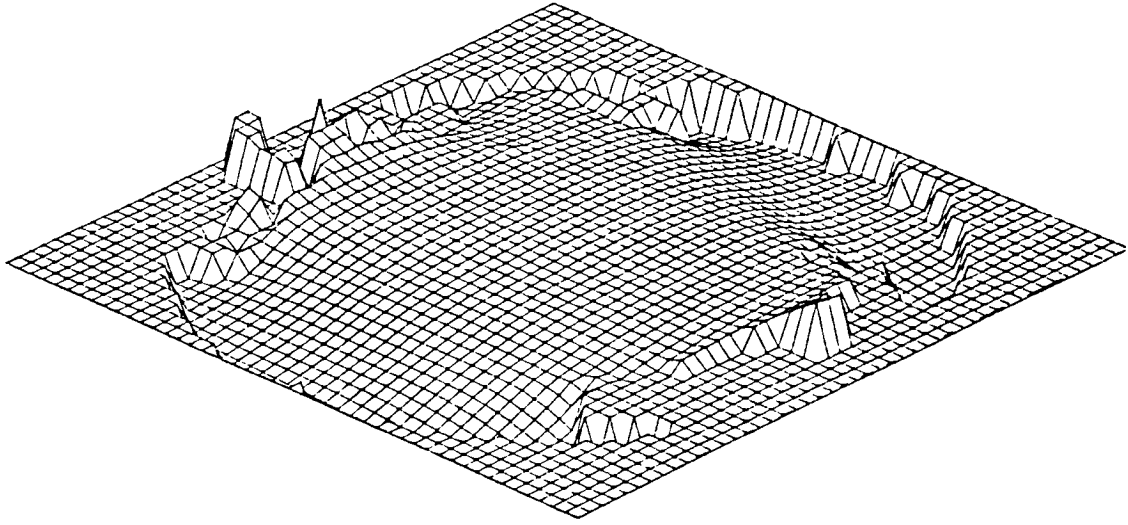
FIGURE 16.  Aperture Phase Distribution after the
Fourth Iteration
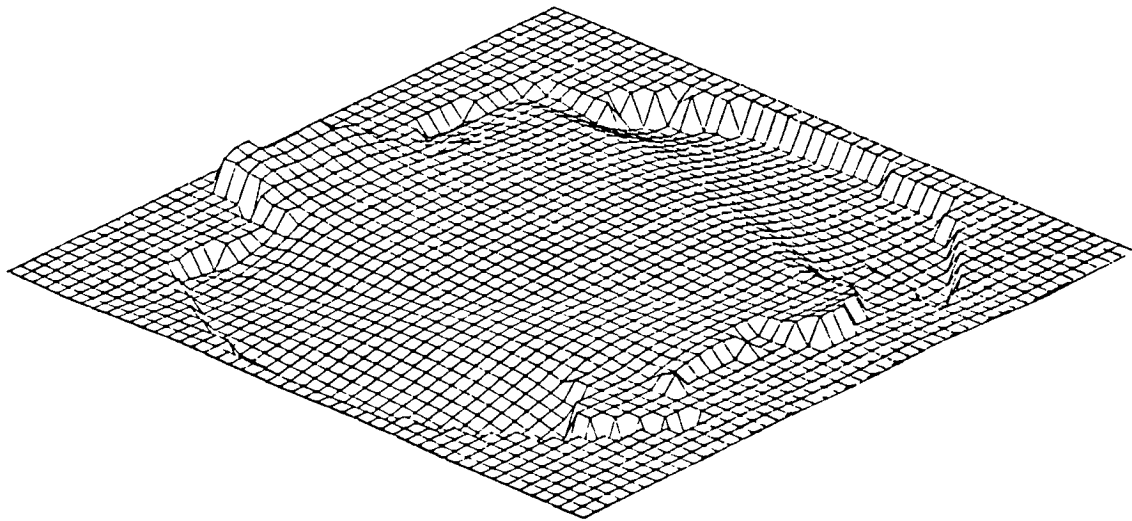
FIGURE 17. A Plot of the Difference (in z Values) Between
the Shaped Reflector Surface and the Initial
Parabolic Reflector Surface. The shaped surface
data was interpolated on a uniform x-y grid from the
randomly spaced data obtained from the numerical results.
The peak to peak variation is about 0.5 λ
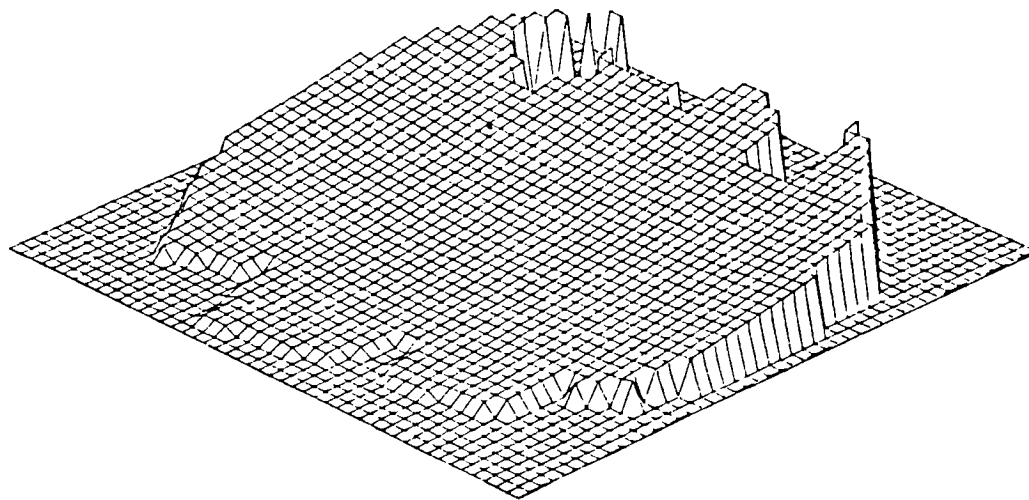
FIGURE 18. The Shaped Reflector Surface
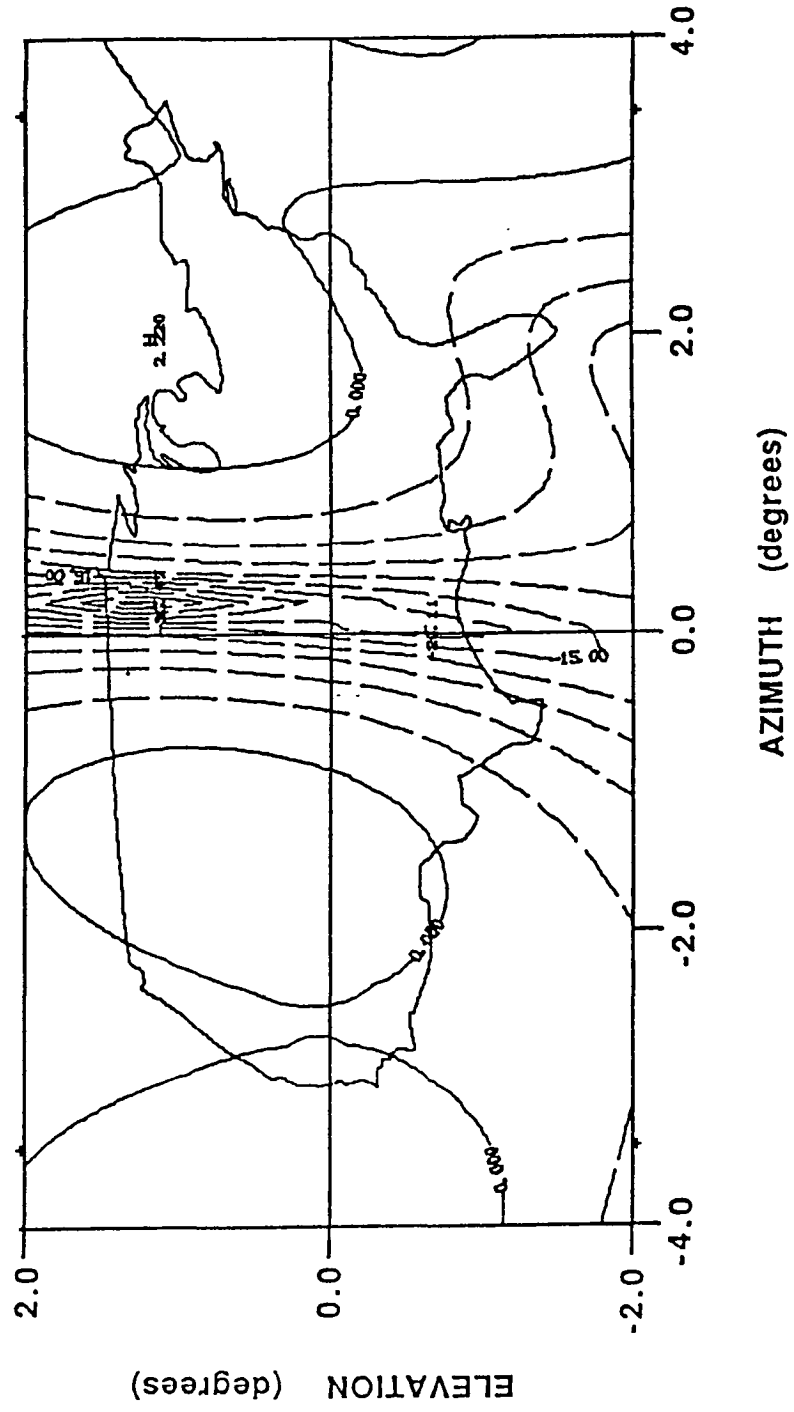
FIGURE 19. Cross Polarization Pattern for the Shaped Reflector after the Fouth Iteration
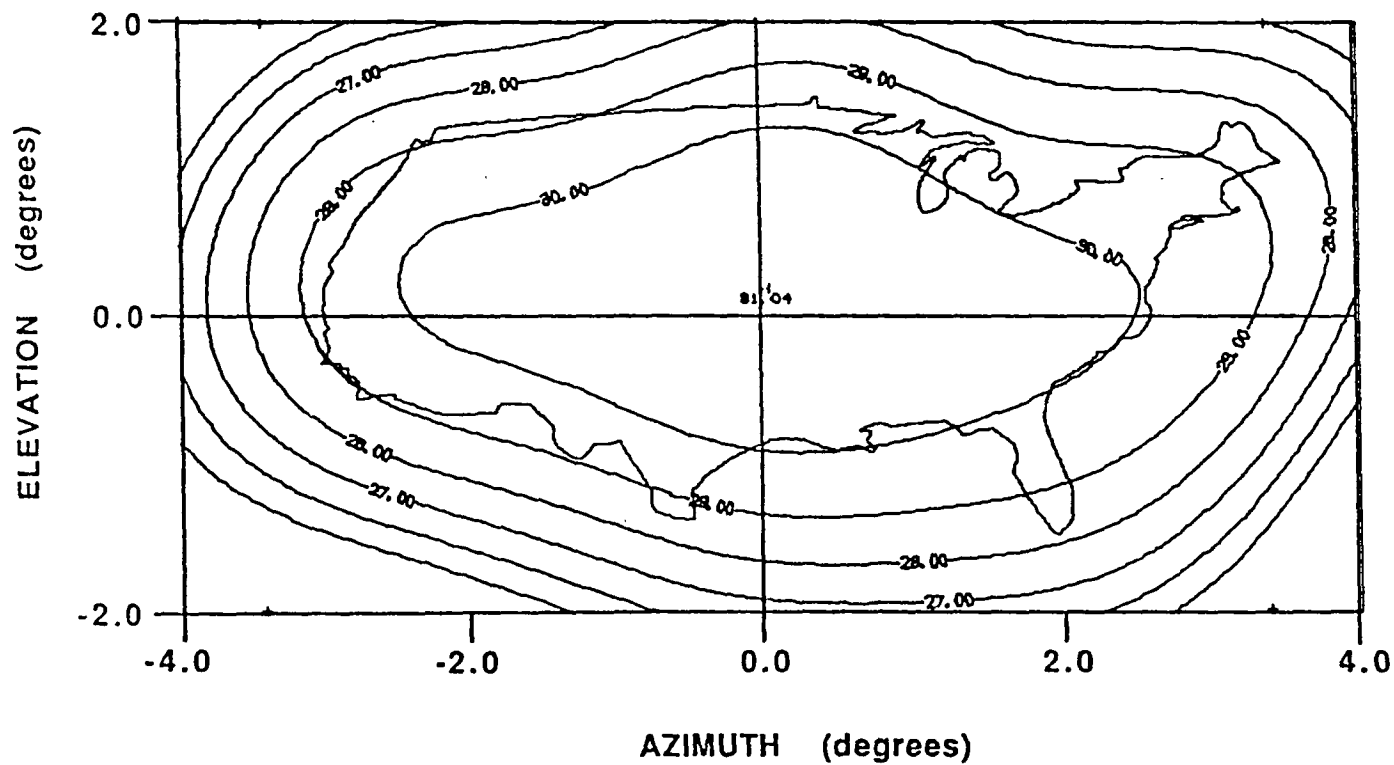
**FIGURE 20. Physical Optics Farfield Pattern for the Shaped Reflector.**
The pattern was calculated using physical optics and the
interpolated reflector surface after the fourth iteration.

# NASA
National Aeronautics and
Space Administration

# Report Documentation Page

| 1 Report No. | 2. Government Accession No. | 3. Recipient's Catalog No. |
|---|---|---|
| NASA TM-101369 | | |

| 4. Title and Subtitle | | 5. Report Date |
|---|---|---|
| A Method for Producing a Shaped Contour Radiation Pattern Using a Single Shaped Reflector and a Single Feed | | October 1988 |
| | | 6. Performing Organization Code |

| 7. Author(s) | 8. Performing Organization Report No. |
|---|---|
| A.R. Cherrette, S.W. Lee, and R.J. Acosta | E-4408 |
| | 10. Work Unit No. |
| | 650-60-20 |

| 9. Performing Organization Name and Address | 11. Contract or Grant No. |
|---|---|
| National Aeronautics and Space Administration Lewis Research Center Cleveland, Ohio 44135-3191 | |
| | 13. Type of Report and Period Covered |

| 12. Sponsoring Agency Name and Address | Technical Memorandum |
|---|---|
| National Aeronautics and Space Administration Washington, D.C. 20546-0001 | 14. Sponsoring Agency Code |

15. Supplementary Notes

16. Abstract

Eliminating the corporate feed network in shaped contour beam antennas will reduce the expense, weight, and RF loss of the antenna system. One way of producing a shaped contour beam without using a feed network is to use a single shaped reflector with a single feed element. For a prescribed contour beam and feed, an optimization method for designing the reflector shape is given. As a design example, a shaped reflector is designed to produce a continental U. S. coverage (CONUS) beam. The RF performance of the shaped reflector is then verified by physical optics.

| 17. Key Words (Suggested by Author(s)) | 18. Distribution Statement |
|---|---|
| Antenna radiation patterns Shaped beam Contour radiation pattern | Unclassified – Unlimited Subject Category 32 |

| 19. Security Classif. (of this report) | 20. Security Classif. (of this page) | 21 No of pages | 22. Price* |
|---|---|---|---|
| Unclassified | Unclassified | 44 | A03 |

NASA FORM 1626 OCT 86   *For sale by the National Technical Information Service, Springfield, Virginia 22161